ARMY RESEARCH LABORATORY

Extensive Characterization of Cracking in As-fabricated Composite Ceramic Panels Via Ultrasonic and X-ray Computed Tomography Testing

by William H. Green and Raymond E. Brennan

ARL-TR-5638 **August 2011**

NOTICES

Disclaimers

Army Research Laboratory

Aberdeen Proving Ground, MD 21005-5069

ARL-TR-5638 **August 2011**

Extensive Characterization of Cracking in As-fabricated Composite Ceramic Panels Via Ultrasonic and X-ray Computed Tomography Testing

William H. Green and Raymond E. Brennan
Weapons and Materials Research Directorate, ARL

REPORT DOCUMENTATION PAGE			*Form Approved* *OMB No. 0704-0188*

1. REPORT DATE *(DD-MM-YYYY)*	August 2011
2. REPORT TYPE	Final
3. DATES COVERED (From - To)	April 20 to August 20, 2010
4. TITLE AND SUBTITLE	Extensive Characterization of Cracking in As-fabricated Composite Ceramic Panels Via Ultrasonic and X-ray Computed Tomography Testing
5a. CONTRACT NUMBER	
5b. GRANT NUMBER	
5c. PROGRAM ELEMENT NUMBER	
6. AUTHOR(S)	William H. Green and Raymond E. Brennan
5d. PROJECT NUMBER	
5e. TASK NUMBER	
5f. WORK UNIT NUMBER	
7. PERFORMING ORGANIZATION NAME(S) AND ADDRESS(ES)	U.S. Army Research Laboratory ATTN: RDRL-WMM-D 4600 Deer Creek Loop Aberdeen Proving Ground, MD, 21005-5069
8. PERFORMING ORGANIZATION REPORT NUMBER	ARL-TR-5638
9. SPONSORING/MONITORING AGENCY NAME(S) AND ADDRESS(ES)	
10. SPONSOR/MONITOR'S ACRONYM(S)	
11. SPONSOR/MONITOR'S REPORT NUMBER(S)	
12. DISTRIBUTION/AVAILABILITY STATEMENT	Approved for public release; distribution unlimited.
13. SUPPLEMENTARY NOTES	

14. ABSTRACT

Decreasing the weight of protective systems, while minimizing the decrease in ballistic performance, is an ongoing goal of the Army. Ceramic materials are currently combined with other materials in these types of structures in order to decrease weight without losing ballistic performance. This includes structures in which the ceramic material is confined in some way or completely encapsulated. Confinement or encapsulation of ceramic material within a structure generally adds complexity and cost. Relatively simple panel specimens fabricated with ceramic tiles on aluminum backings and side confinement using steel were evaluated using nondestructive methods, including x-ray computed tomography and ultrasonic testing. The nondestructive evaluation results are discussed and compared, including the detectability and mapping of the fabrication features.

15. SUBJECT TERMS

X-ray computed tomography, ultrasonic testing, protective system, nondestructive evaluation, ceramics, fabrication flaws

16. SECURITY CLASSIFICATION OF:			17. LIMITATION OF ABSTRACT	18. NUMBER OF PAGES	19a. NAME OF RESPONSIBLE PERSON
a. REPORT	b. ABSTRACT	c. THIS PAGE			William H. Green
Unclassified	Unclassified	Unclassified	UU	22	19b. TELEPHONE NUMBER (*Include area code*) (410) 306-0817

Standard Form 298 (Rev. 8/98)
Prescribed by ANSI Std. Z39.18

Contents

List of Figures

1. Introduction

Nondestructive evaluation (NDE) or nondestructive testing (NDT) is a discipline of materials science that encompasses a wide variety of inspection modalities. NDE is applicable to an extremely wide variety of materials, components, and systems and is used to inspect objects at the surface and sub-surface, and in the interior. Two methods used for the evaluation and analysis of internal geometrical and physical characteristics of materials are x-ray computed tomography (XCT) and ultrasonic testing (UT) or scanning. Both of these methods have been used to characterize armor ceramics, including ballistically damaged ceramics (*1–5*), and XCT has been used to characterize and evaluate ballistically damaged encapsulated ceramic panels (*6*). Ceramic materials are currently combined with other materials in armor panel structures in order to decrease weight without losing ballistic performance. Panels in which the ceramic material is surrounded or completely encapsulated and backed by a supporting material are an example of this approach. However, the higher the degree and sophistication of encapsulation is the higher the complexity of fabrication is. Two simple ceramic panel specimens, which had side confinement of the ceramic tile using steel, were characterized and evaluated using UT and XCT.

2. Description of Specimens and Digital Radiography Scans

Each of the two specimens consists of a 4 in x 4 in x 0.50 in boron carbide (B_4C) tile surrounded by four 5 in x 1 in x 0.50 in pieces of steel all bonded onto a 6 in x 6 in x 0.87 in aluminum backing plate. The four pieces of steel were placed such that each one extended 1 in past the side of the tile in a wraparound surround. Digital radiographs (DRs) of each specimen were taken through their thickness using the 420 keV x-ray tube and linear detector array (LDA) setup in centered rotate-only (RO) mode. The x-ray technique parameters of the DRs were 400 keV and 2.0 mA and the geometry of the source-to-object-distance (SOD) was 750.00 mm and the source-to-image-distance (SID) was 940.00 mm. Figure 1 shows DRs of each specimen, in which the gray-shaded tiles are in the center and the steel surround pieces around the tile are white. This is because the steel attenuates the x-rays significantly more than the tile and aluminum. The DR of the first specimen (figure 1a) shows no cracks in the tile and no gaps between the sides of the tile and the steel surround. The lighter blotchy area in the center of the tile is due to material that was on the rear of the aluminum backing. The slight vertical banding is an image artifact (i.e., not physically in the specimen) due to offset and gain (window) adjustment to optimize image detail. The DR of the second specimen (figure 1b) shows cracks in the tile and a significant gap, which gets larger towards the top of the image, between the side of the tile and the vertical right surround piece. The cracks extend to the vicinity of the upper two and lower right corners of the

tile, with a fainter indication extending to the lower left corner. The DR clearly shows the tilt of the vertical right surround piece.

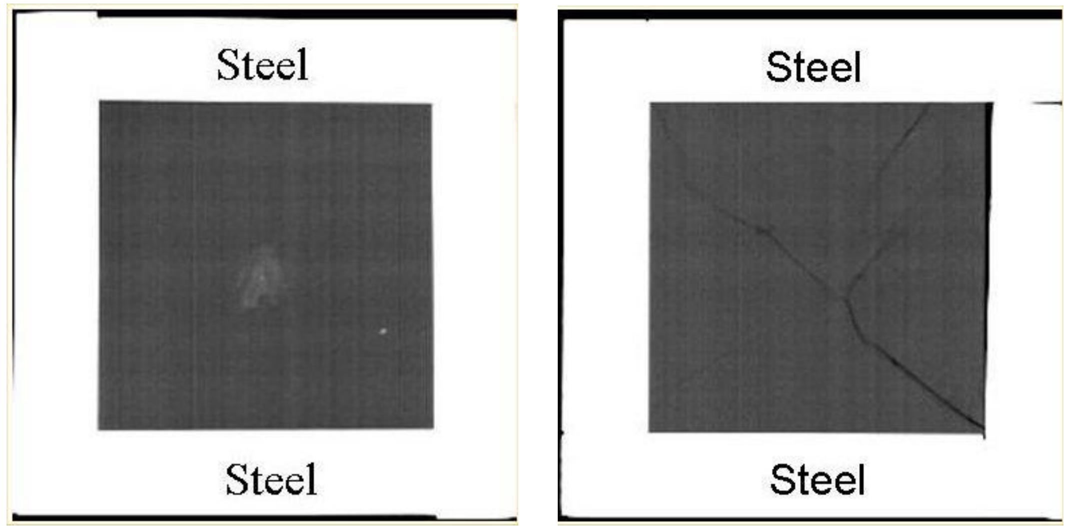

(a) (b)

Figure 1. Through-thickness DRs: (a) specimen number 1 and (b) specimen number 2.

3. XCT and UT Scanning Procedures

Each specimen was placed and stabilized on the turntable with its faces in a vertical orientation for XCT scanning. Thus, the specimen faces were perpendicular to the horizontal x-ray (collimated) fan beam, resulting in through-thickness cross-sectional images. Approximately the middle vertical 100 mm of each specimen from the bottom to the top of the tiles was scanned. Each specimen was scanned using the 420-keV x-ray tube and LDA set up in offset RO mode. The scans were overlapping with a slice thickness and increment of 1.000 and 0.900 mm, respectively, and each slice was reconstructed to a 1024 by 1024 image matrix. The field of reconstruction (FOR) diameter was 175.00 mm. The tube energy and current used were 400 keV and 2.0 mA, respectively, and the focal spot was 0.80 mm. The SOD and SID were 750.00 mm and 940.00 mm, respectively.

Each specimen was also ultrasonically scanned using a phased array pulse-echo immersion (water) setup. As the acoustic waves were transmitted into the specimens, material changes in the components (pores, cracks in the tiles) resulted in acoustic impedance mismatches that caused reflection of the waves (*7*, *8*). The reflected acoustic waves were selected, gated, and collected as a function of signal amplitude, or intensity. Reflected signals from the top surface of the specimens were used to collect surface/near-surface data while bottom surface reflected signals were used to collect bulk data through each specimen. Spatial maps, or ultrasound C-scan images, of the gated signals were used to form visual plots of acoustic variations caused

by defects and/or fabrication damage. Testing was conducted using a 64-element, 10-MHz linear phased array transducer. A total of 32 active elements were used for each scan, with active area dimensions of 32.0 mm length, 0.5 mm pitch, and 7.0 mm elevation. The transducer was mounted to a scanning bridge for motion control in the *x*-, *y*-, and *z*-axes during setup and testing.

4. Evaluation of As-fabricated Specimens

4.1 Specimen Number 1

4.1.1 Ultrasonic Scans

Figure 2 shows three ultrasonic variable amplitude C-scans in which the up direction from the bottom of the images corresponds to increasing z in the DR scan of the specimen. The scan in figure 2a was gated to show the front surface and near surface characteristics of the specimen and indicates two major cracks in the tile. The scan in figure 2b was gated to show only the signal amplitude at the rear surface of the tile. The scan in figure 2c was gated to show the overall bulk characteristics of the tile. Both of the images in 2b and 2c show widespread attenuation, indicated by the darker areas, most likely due to cracks within the tile. Figure 3 shows a through-thickness B-scan presentation of the specimen going from left to right approximately halfway between the bottom and top of the tile. The B-scan view shows the ultrasonic amplitude against time (i.e., depth), which is on the *y*-axis, over the length of the line (horizontal) defining the cross-sectional location. The physical side locations of the steel surround pieces are marked and the vertically larger white areas (e.g., left side) indicate more immediate loss of signal. The B-scan clearly shows where cracking damage is resulting in relatively fast signal attenuation, including much of the left side, the center area, and part of the right side.

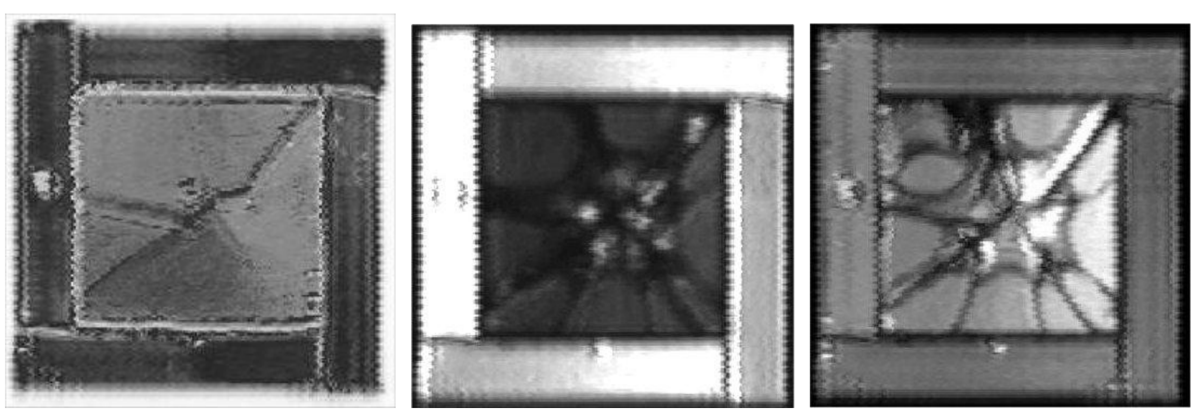

(a) (b) (c)

Figure 2. Ultrasonic C-scans of specimen 1: (a) surface/near-surface of specimen, (b) rear surface of tile signal amplitude only, and (c) bulk characteristics of tile.

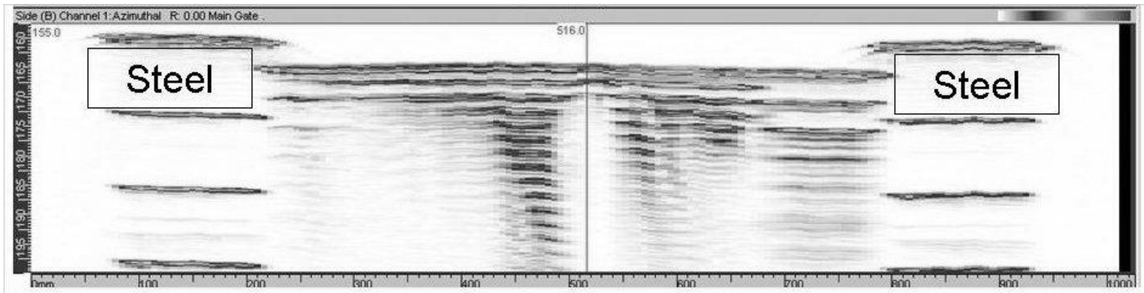

Figure 3. Through-thickness, or depth, B-scan presentation of specimen 1 going from left to right approximately halfway between the bottom and top of the tile. The physical side locations of the steel surround pieces are marked.

4.1.2 Computed Tomography Scans

Figure 4 shows a representative XCT scan (image) of the specimen in which the aluminum backing plate and steel surround pieces are labeled. The front surface of the tile is located at the top of the image. The darkened cross pattern in the tile is due to a combination of the location of the steel in relation to the tile and significantly greater x-ray attenuation by the steel as compared to the tile. The image does not show indications of cracks. This is most likely due to some combination of the difficulty in image interpretation caused by the cross pattern artifact and very tight cracks with small or no gaps (i.e., “kissing” cracks).

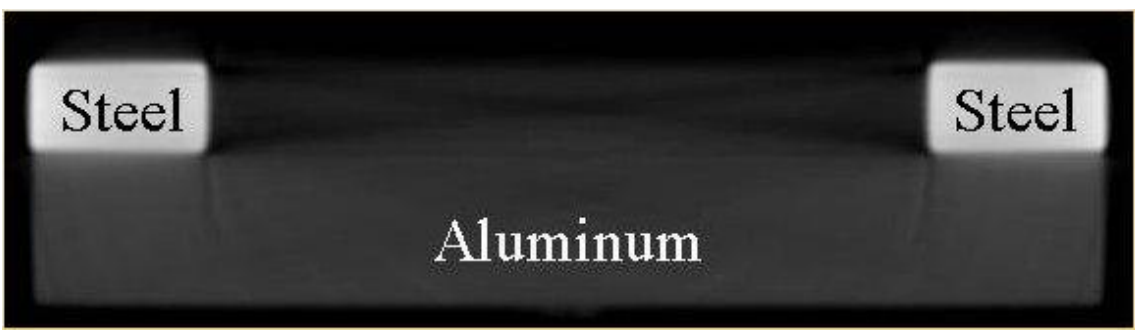

Figure 4. Representative XCT scan (image) of specimen 1 with locations of steel surround pieces and aluminum backing plate labeled. Note the darkened cross pattern artifact between the pieces of steel.

4.2 Specimen Number 2

4.2.1 Ultrasonic Scans

Figure 5 shows three ultrasonic variable amplitude C-scans in which the up direction from the bottom of the images corresponds to increasing z in the DR scan of the specimen. The scan in figure 5a was gated to show the front surface and near surface characteristics of the specimen and indicates at least five major cracks in the tile. The scan in figure 5b was gated to show only the signal amplitude at the rear surface of the tile. The scan in figure 5c was gated to show the overall bulk characteristics of the tile. Both of the images in 5b and 5c show widespread

attenuation, indicated by the darker areas, most likely due to cracks within the tile. Figure 6 shows a through-thickness B-scan presentation of the specimen going from left to right approximately halfway between the bottom and top of the tile. The B-scan view shows the ultrasonic amplitude against time (i.e., depth), which is on the *y*-axis, over the length of the line (horizontal) defining the cross-sectional location. The physical side locations of the steel surround pieces are marked and the vertically larger white areas indicate more immediate loss of signal. The B-scan clearly shows where cracking damage is resulting in relatively fast signal attenuation, which occurs over the majority of the cross section.

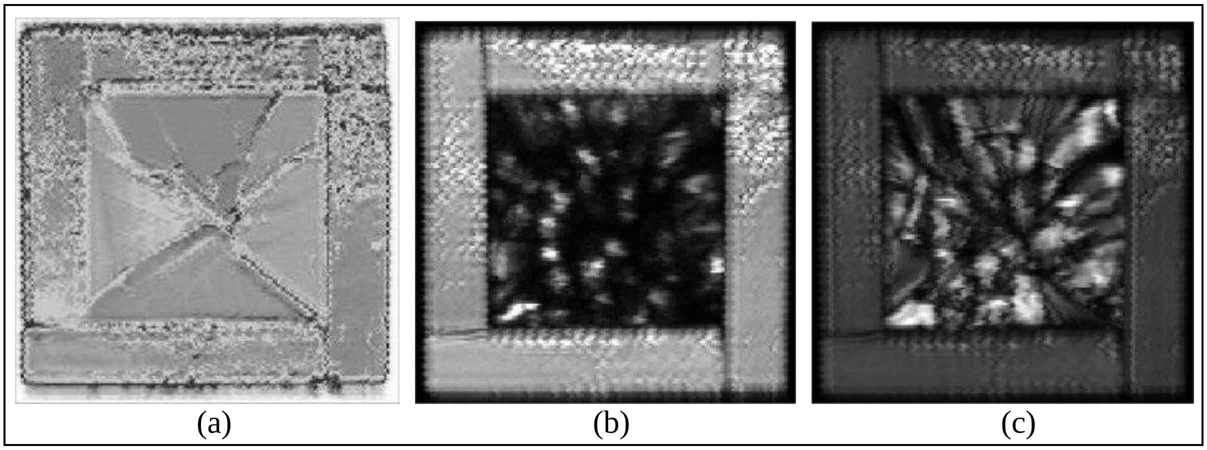

Figure 5. Ultrasonic C-scans of specimen 2: (a) surface/near-surface of specimen, (b) rear surface of tile signal amplitude only, and (c) bulk characteristics of tile.

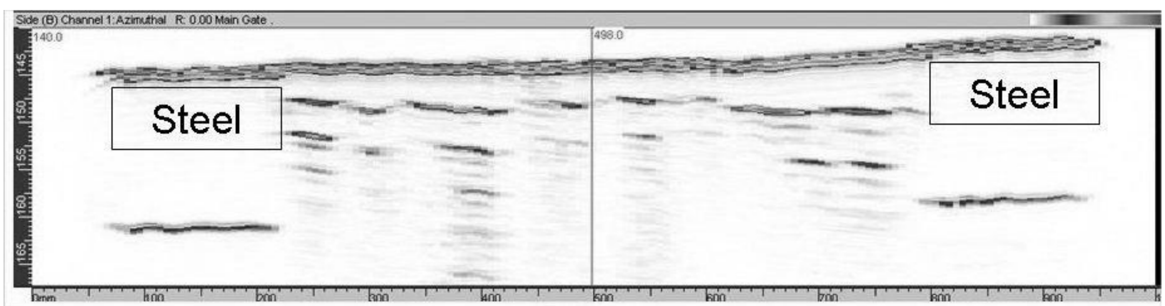

Figure 6. Through-thickness, or depth, B-scan presentation of Specimen 2 going from left to right approximately halfway between the bottom and top of the tile. The physical side locations of the steel surround pieces are marked.

4.2.2 Computed Tomography Scans

The vertical positions (z-direction) of the bottom and top of the tile were 330.5 and 432.0 mm, respectively, in the XCT scans. Figure 7 shows a series of XCT scans (images) of the specimen at vertical positions of 339.70, 353.20, 382.90, 395.50, 413.50, and 431.50 mm (a–f). The front surface of the tile is at the top of the images. The presence of cracking in the tile is evident near its bottom on the right side as shown in figure 7a. The cracking continues to extend into the interior and towards the front of the tile as the positions of the scans increase, finally reaching

from one rear side corner to the other. Other cracks approximately perpendicular to the faces of the tile also extend from this main feature to the front of the tile. The image at a height of 431.50 mm (f) also shows that part of the rear face of the tile on the right has come away from the backing plate and is no longer in intimate contact with the plate. This is the same side of the tile adjacent to which the tilted steel surround piece is located. It is evident that the crack enters the interior of the tile at the juncture between contact and stand off of the rear face of the tile with the backing plate.

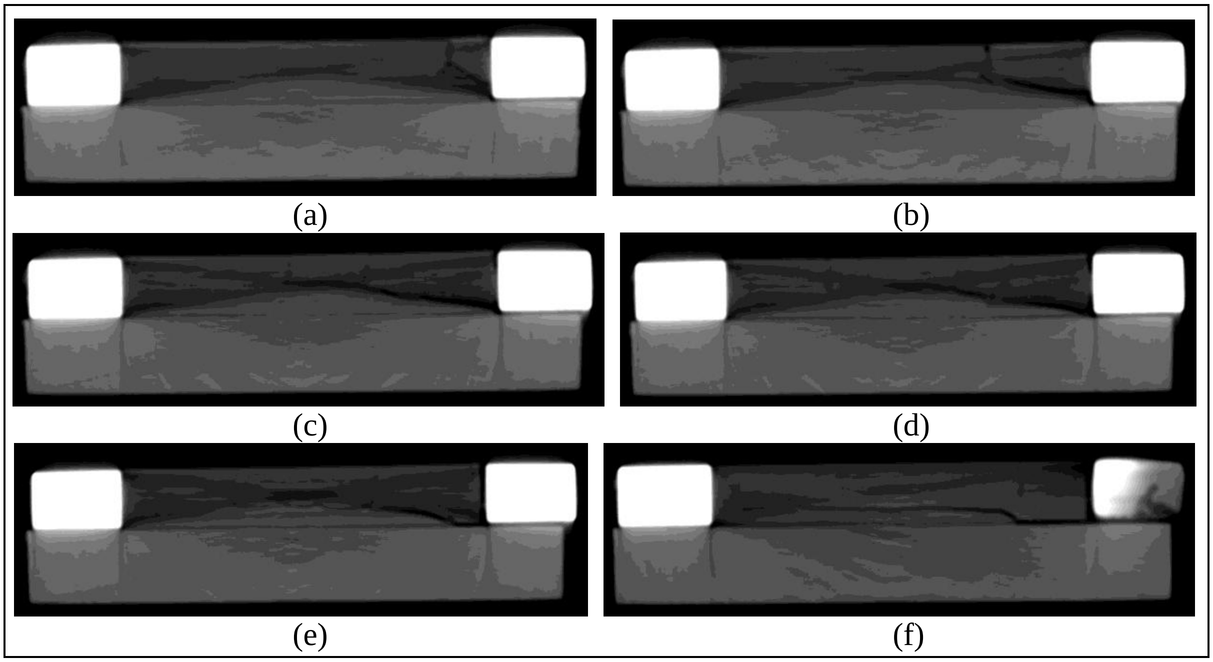

Figure 7. A series of cross-sectional XCT scans (images) of specimen 2: scans (a–f) were taken at vertical positions of 339.70, 353.20, 382.90, 395.50, 413.50, and 431.50 mm, respectively.

4.2.3 Three-dimensional Solid Visualization

The excellent dimensional accuracy and the digital nature of XCT images allow the accurate volume reconstruction of multiple adjacent or overlapping slices. A virtual three-dimensional (3-D) solid image is created by electronically stacking the XCT images, which have thickness over their cross sections (i.e., voxels), one on top of the previous from the bottom to the top of the specimen or scanned height to generate its virtual volume. Figure 8 shows a series of 3-D solid images of the scanned volume with sections virtually removed in figure 8b–f. The method of virtual sectioning, which is essentially only showing a portion of each scan, allows viewing of generated surfaces anywhere in the scanned volume in 3-D space. The view in figures 8a, 8b, 8e, and 8f is looking at the front of the specimen with it tilted forward. In figures 8c and 8d, the specimen has been tilted forward as well as rotated in order to better view the side sections. Figure 8a shows the entire scanned volume with surfaces and no sections virtually removed. In figure 8b, approximately the right-hand side of the specimen has been virtually removed. The main lateral crack near the rear of the tile is visible, as are some perpendicular cracks that go to

the front surface of the tile. In figure 8c, approximately the top half of the specimen has been virtually removed. It shows cracking at about the middle of and to the right in the sectioned surface, as well as the connections between the crack indications on the front surface and the interior cracks perpendicular to the surfaces. In figure 8d, approximately the top half as well as a smaller section on the right-hand side of the specimen has been removed. The connection of the cracks from one sectioned surface into the adjacent sectioned surface at the intersection (edge) of the two surfaces is evident. In figure 8e, a few millimeters of material in the thickness direction parallel to the faces of the tile has been removed from the front of the specimen. The crack pattern looks similar to the crack pattern on the surface of the tile (figure 8a). In figure 8f, about half of the thickness of the tile has been removed. More severe damage in the center region where the cracks come together, as well as in the lower right area, is evident. The vertical darker broad band in the center of the tile is the manifestation of the relative attenuation effect of the steel as compared to the tile (and aluminum).

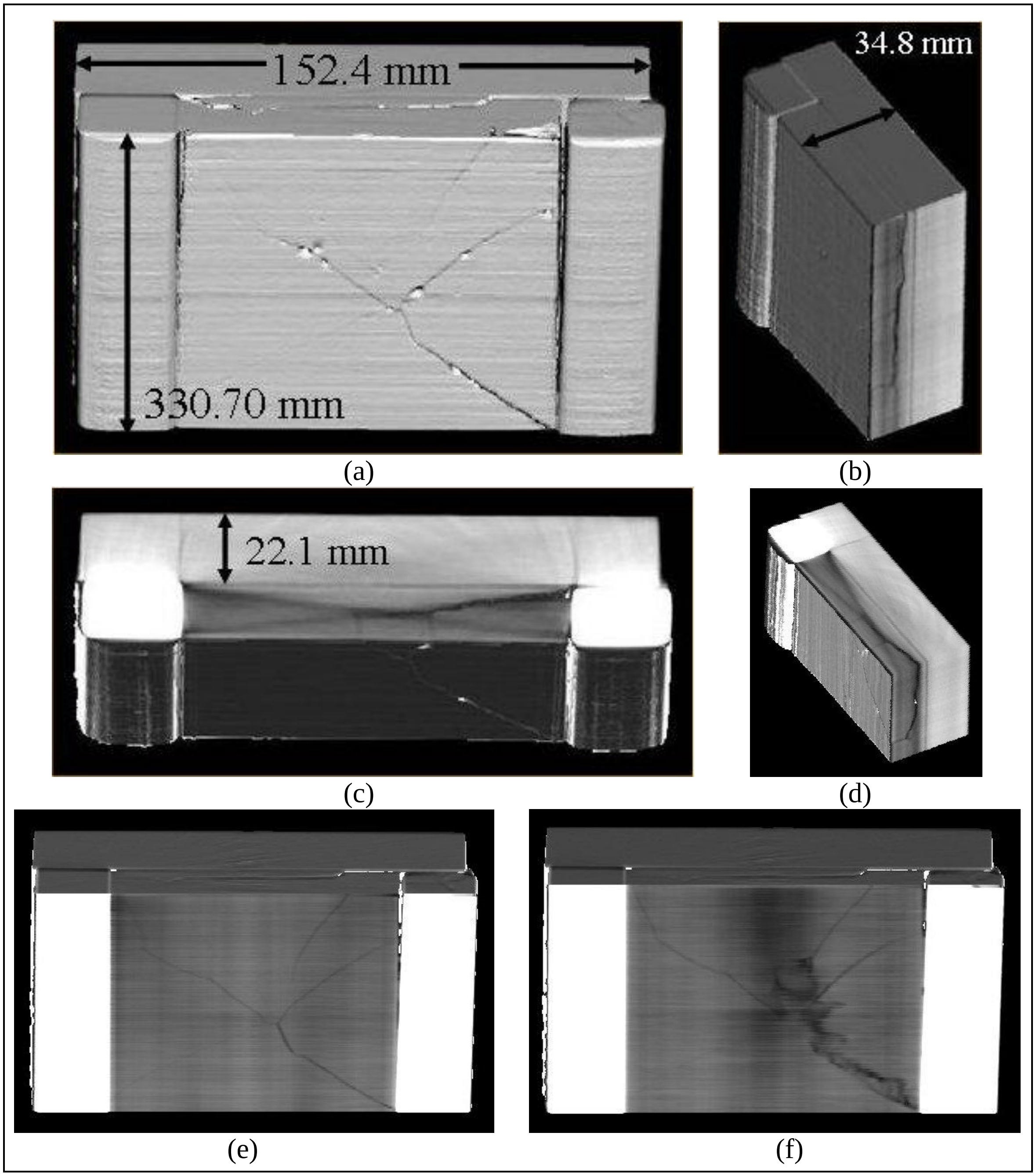

Figure 8. A series of 3-D solid visualization images of specimen 2: (a) entire specimen with the front tilted forward, (b) section removed perpendicular to thickness, (c) section removed perpendicular to height. (d) sections removed perpendicular to both thickness and height, (e) section removed parallel to the faces showing the majority of thickness of the tile, and (f) section removed parallel to the faces showing about half the thickness of the tile.

4.2.4 Three-dimensional Point Cloud and Feature Visualization

A 3-D point cloud is a set of points in space that define geometrical characteristics (i.e., shape, size, location) of a specimen or scanned volume and features within it. Location of the points is routinely determined by appropriate (image) segmentation of the feature or features of interest. However, if image artifacts are severe enough, they can make it very difficult, if not impossible, to determine and apply a segmentation approach using only a single (gray) level. Figure 9 shows the XCT image of the specimen at a height of 382.90 mm, in which the critical locations defining the beginning and terminating points of the cracks are individually marked. Each point is listed below the image on the left in (x, y, z) format, as well as the points for the same cracks at a different vertical location on the right. This approach was used because single-level segmentation was not successful with these images. The beginning and terminating points of the cracks in each XCT image were determined and used to directly create a point cloud showing each cracks location and orientation. The points defining the lower and upper corners of the steel surround pieces and aluminum backing plate in the scanned volume were also determined.

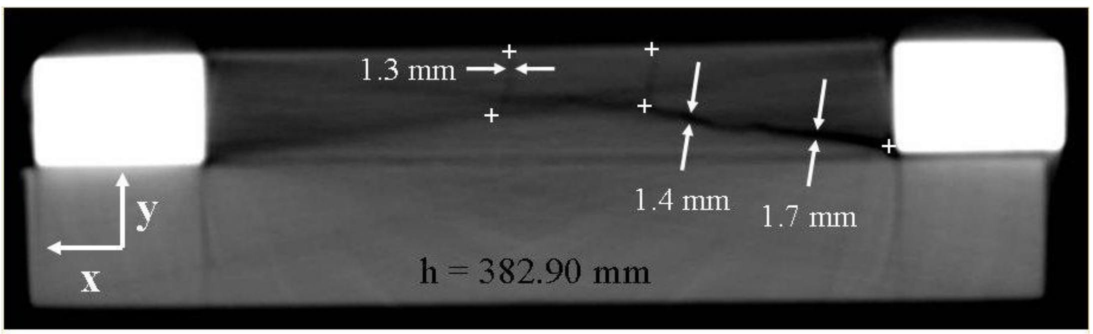

. . . . .	(-54.17, 2.99, 382.90)	(-53.83, 2.65, 384.70)	. . . . .
. . . . .	(-16.75, 8.80, 382.90)	(-18.12, 8.63, 384.70)	. . . . .
. . . . .	(-18.97, 17.86, 382.90)	(-20.51, 17.60, 384.70)	. . . . .
. . . . .	(4.53, 8.12, 382.90)	(6.15, 8.03, 384.70)	. . . . .
. . . . .	(3.33, 17.69, 382.90)	(5.21, 17.60, 384.70)	. . . . .

Figure 9. XCT scan (image) at vertical height of 382.90 mm and defining spatial locations of crack planes.

Figure 10 is an isometric view of the scanned volume of the specimen, in which the edges of each component are shown in wire frame mode and dashed lines indicate rear or blocked view edges. The points defining the crack locations and orientations are shown within the body of the tile. The tilted steel surround piece is on the right side of the image. Figure 11 is an isometric view of the scanned volume showing the points and the boundary curves that were fit to the points. Figure 12 is an isometric view of the scanned volume showing only the boundary curves within the body of the tile. Figure 13 is an isometric view of the scanned volume showing gridded surfaces fit to the boundary curves defining major crack regions and their interconnection. Figure 14 is an isometric view of the scanned volume showing shaded surfaces

fit to the boundary curves defining major crack regions and their interconnection, as well as other crack plane features. The parallel gray lines drawn in the top of the tile indicate that there is also a crack plane in the region spanned by them. Secondly, the relatively faint crack indication in the lower left area of the DR of the specimen is marked by the two parallel arrows in the lower left part of the body of the tile. Figure 15 is an isometric view of the tile only showing the various crack regions, indicating that a significant volume of the tile is severely cracked. This volumetric representation of the damage also clearly shows that the crack regions go from both side-to-side and bottom-to-top in the body of the tile.

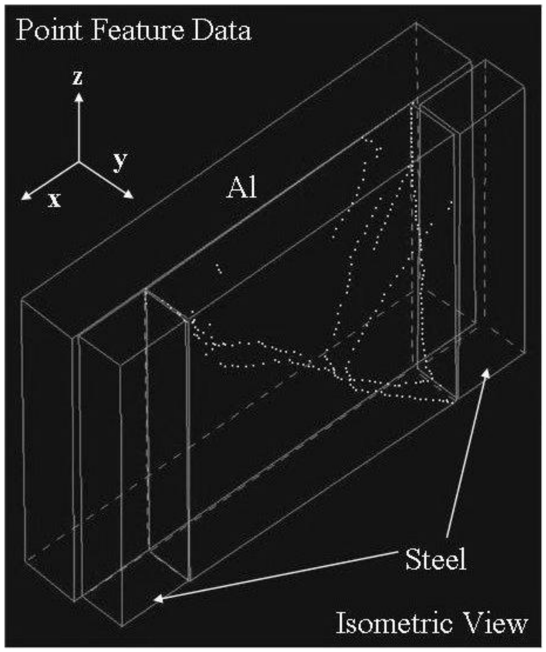

Figure 10. 3-D point cloud of the defining locations of the crack planes.

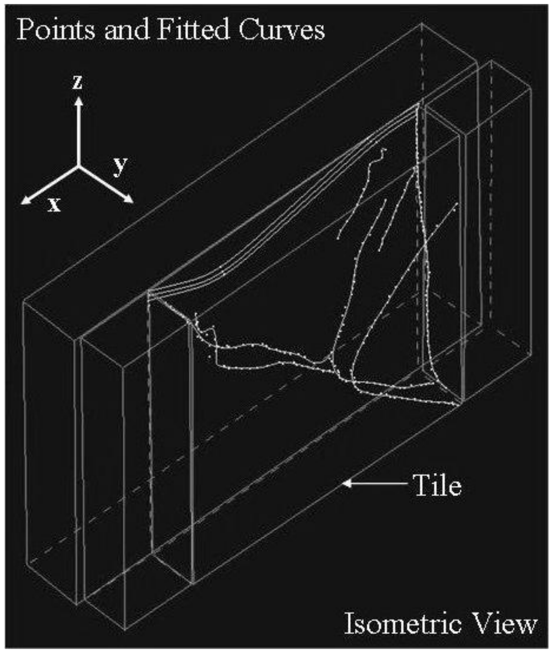

Figure 11. 3-D point cloud and boundary curves of the crack planes.

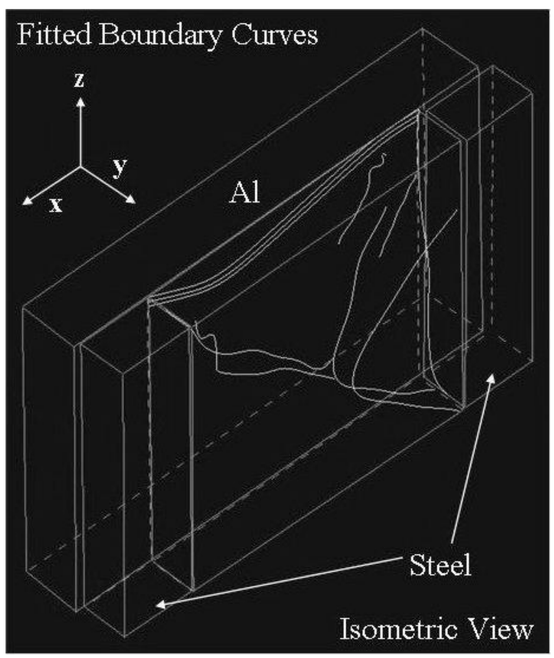

Figure 12. Boundary curves of the crack planes.

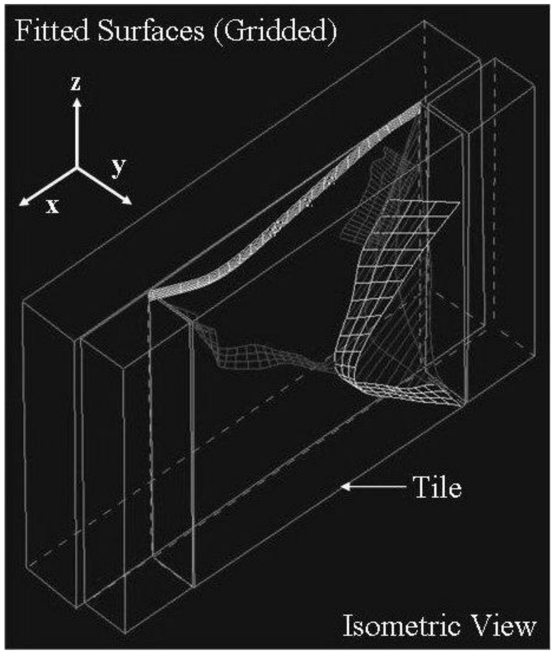

Figure 13. Fitted crack plane surfaces (gridded).

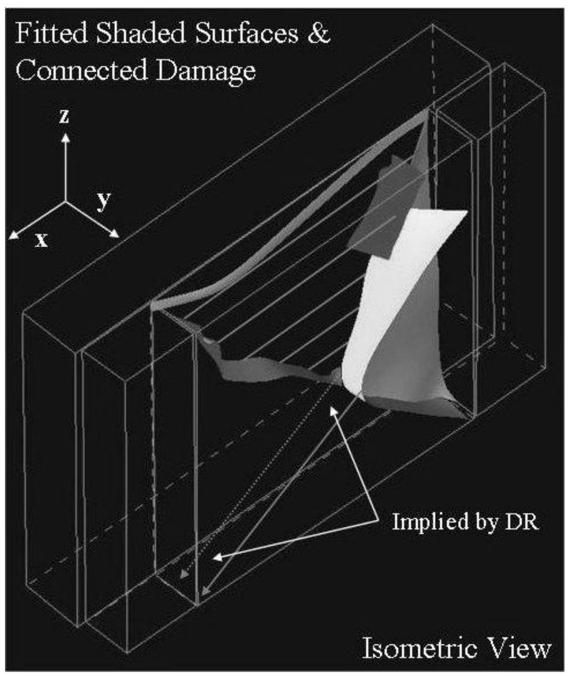

Figure 14. Crack plane surfaces showing the entire specimen.
The tilted steel piece is on the right.

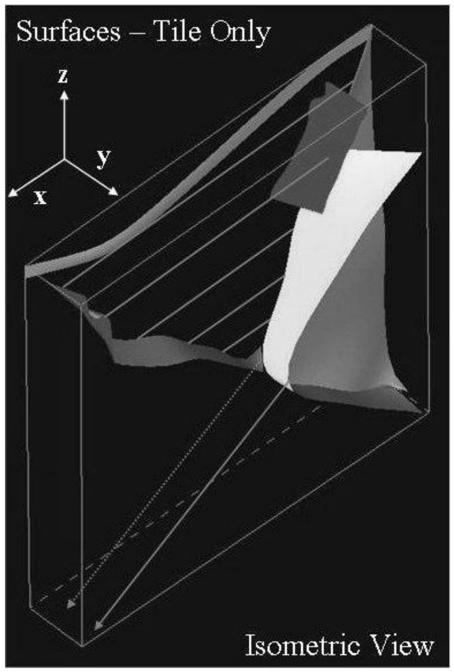

Figure 15. Crack plane surfaces showing the tile only.

5. Conclusions

Fabrication features and damage in two 6 in x 6 in ceramic modules made with 4 in x 4 in ceramic tiles, aluminum backing plates, and four-piece steel side surrounds (“wrap around” construction) were characterized using UT and XCT analysis. The ultrasonic scans of specimen 1 indicated significant attenuation within the tile, most likely due to cracking. The XCT scans did not show indications of cracks, probably due to the combination of the interpretation difficulty from the presence of the cross pattern artifact and very tight cracks with small or no gaps. We captured and discussed features and damage including misaligned surround pieces; gaps between surround pieces and the tile; extensive cracking in general; and cracking in and standoff of the rear of the tile in specimen 2. Successive application of XCT 2-D evaluation, volumetric solid visualization and analysis, and volumetric point feature data combined with curve and damage surface visualization provided extensive qualitative and quantitative data about the spatial distribution of crack damage in the specimen. Comparison of the UT and XCT images of the two specimens indicates that the effectiveness of the physical confinement influences the presence and severity of fabrication discontinuities, or flaws. Characteristics of captured features and damage in the tiles provided better understanding of the physical behavior of the modules under fabrication conditions.

6. References

1. Green, W.; Miller, H.; LaSalvia, J.; Dandekar, D.; Casem, D. Evaluation of Ballistically-induced Damage in Ceramic Targets by X-ray Computed Tomography. *Proceedings of 32nd International Conference on Advanced Ceramics and Composites - Topics in Ceramic Armor*, 2008.

2. Green, W.; Rupert, N.; Wells, J. Inroads in the Non-invasive Diagnostics of Ballistic Impact Damage. *Proceedings of 25th Army Science Conference*, 2006.

3. Miller, H.; Green, W.; LaSalvia, J. Ballistically-induced Damage in Ceramic Targets as Revealed by X-ray Computed Tomography. *Proceedings of 31st International Conference on Advanced Ceramics and Composites - Topics in Ceramic Armor*, 2007.

4. Bourne, N.; Green, W.; Dandekar, D. On the One-dimensional Recovery and Microstructural Evaluation of Shocked Alumina. *Proceedings of the Royal Society A: Mathematical, Physical, and Engineering Sciences*, published online: doi:10.1098/rspa.2006.1713, 2006.

5. Wells, J.; Green, W.; Rupert, N.; MacKenzie, D. Capturing Ballistic Damage as a Function of Impact Velocity in SiC-N Ceramic Targets. *Proceedings of 30th International Conference on Advanced Ceramics and Composites - Advances in Ceramic Armor*, 2006.

6. Green, W.; Carter, R. Evaluation of Ballistic Damage in an Encapsulated Ceramic Panel via X-ray Computed Tomography. *Proceedings of Review of Progress in Quantitative NDE*, 2008.

7. Mix, P. E. *Introduction to Nondestructive Testing*; John Wiley & Sons, pp. 104–153, 1987.

8. Krautkramer, J.; Krautkramer, H. *Ultrasonic Testing of Materials*; Springer-Verlag, 1990.

List of Symbols, Abbreviations, and Acronyms

3-D	three-dimensional
B_4C	boron carbide
DRs	digital radiographs
FOR	field of reconstruction
LDA	linear detector array
NDE	nondestructive evaluation
NDT	nondestructive testing
RO	rotate-only
SOD	source-to-object-distance
SID	source-to-image-distance
UT	ultrasonic testing
XCT	x-ray computed tomography

No. of Copies	Organization
1 ELEC	ADMNSTR DEFNS TECHL INFO CTR ATTN DTIC OCP 8725 JOHN J KINGMAN RD STE 0944 FT BELVOIR VA 22060-6218
3 HCS	US ARMY RSRCH LAB ATTN IMNE ALC HRR MAIL & RECORDS MGMT ATTN RDRL CIO LL TECHL LIB ATTN RDRL CIO MT TECHL PUB ADELPHI MD 20783-1197
1 HCS	US ARMY RSRCH LAB ATTN RDRL SED E S GILMAN ADELPHI MD 20783-1197
6 HCS	US ARMY RSRCH LAB ATTN RDRL-WMM-D WILLIAM H. GREEN RAYMOND E. BRENNAN RDRL-WMM-D ERNEST S. CHIN RICHARD SQUILLACIOTI DOUGLAS J. STRAND RDRL-WMM-C CHARLES G. PERGANTIS APG MD 21005-5069
1 HC	OFFICE OF NAVAL RESEARCH GLOBAL ATTN JOE WELLS, SC.D. ASSOCIATE DIRECTOR FOR MATERIALS SCIENCE & ENGINEERING 86 BLENHEIM CRESCENT UNIT 4540 BOX39 RUISLIP MIDDX HA4 7HB UK
TOTAL:	12 (1 ELEC, 11 HCS)